

Relay recognition of F⁻ and a Nerve-agent Mimic diethyl cyanophosphate in mixed aqueous media: Discrimination of diethyl cyanophosphate and diethyl chlorophosphate by cyclization induced fluorescence enhancement

Avijit Kumar Das^a, Shyamaprosad Goswami*^a, Ching Kheng Quah^b and Hoong-Kun Fun^{b,c}

^aDepartment of Chemistry, Indian Institute of Engineering Science and Technology, Shibpur.

^bX-ray Crystallography Unit, School of Physics, Universiti Sains Malaysia, 11800 USM, Penang, Malaysia.

^cDepartment of Pharmaceutical Chemistry, College of Pharmacy, King Saud University, Riyadh 11451, Saudi Arabia.

1. Calculation of the detection limit	2
2. Concentration vs. Intensity plot.....	3
3. Kinetic behaviour	4-5
4. Partial ¹H-NMR spectra of BBCI with DCP.....	5
5. Characterization spectra of BSNA and BBCI (¹H-NMR, HRMS).....	6-9
6. ¹H-NMR and HRMS spectra of BBCI with DCNP.....	10-11
7. X-ray crystallography.....	12-14

Calculation of the detection limit:

The detection limit (DL) of **BSNA** towards F^- and **BBCI** towards DCNP in emission spectra was determined from the following equation¹:

$$DL = K * Sb_1/S$$

Where $K = 2$ or 3 (we take 2 in this case); Sb_1 is the standard deviation of the blank solution; S is the slope of the calibration curve.

From the graph Fig.S1(a), we get slope = 7404.61 , and Sb_1 value is 10523.06 .

Thus using the formula we have detected the green fluorescence of **BSNA** using minimum $2.84 \mu\text{M}$ TBAF.

From the graph Fig.S1(b), we get slope = 117056.89 , and Sb_1 value is 154622.2 .

Thus using the formula we have detected the green fluorescence of **BBCI** using minimum $3.09 \mu\text{M}$ DCNP.

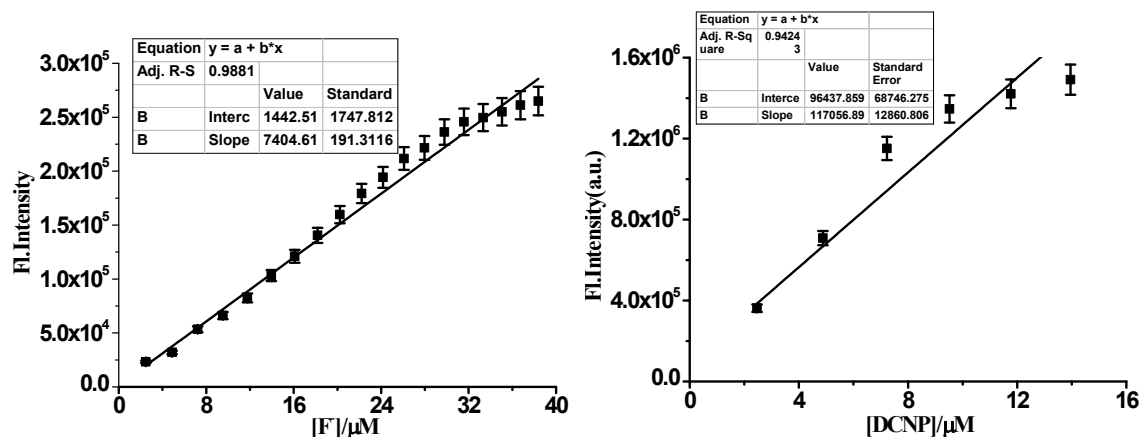


Figure S1: (a) Changes of emission intensity of **BSNA** ($c = 2 \times 10^{-5} \text{M}$) as a function of **[TBAF]** ($c = 2 \times 10^{-4} \text{M}$) at 486 nm . **(b)** Changes of emission intensity of **BBCI** ($c = 2 \times 10^{-5} \text{M}$) as a function of **[DCNP]** ($c = 2 \times 10^{-4} \text{M}$) at 480 nm .

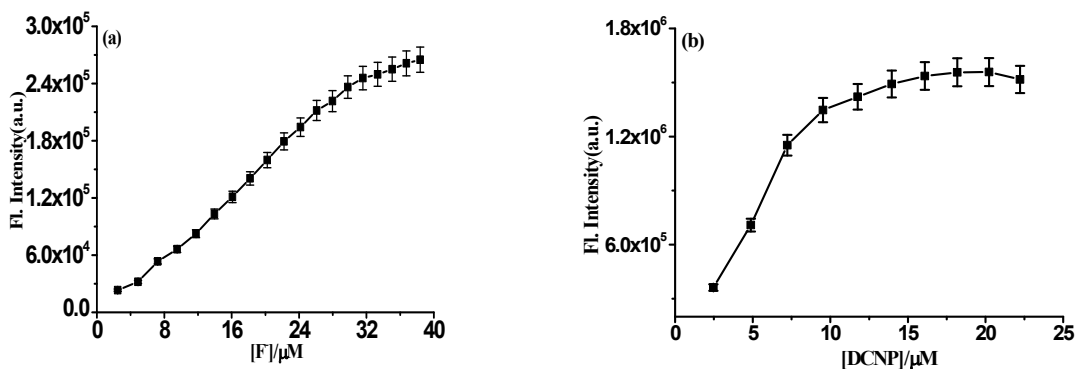


Figure S2: (a) Fluorescence changes of **BSNA** on addition of TBAF. (b) Concentration vs. intensity plot of the fluorescence spectra of isolated de-silylation product of **BSNA** with TBAF (**BBCI**) with DCNP in $\text{CH}_3\text{CN}/\text{H}_2\text{O}$ (5/5, v/v, 25°C) at pH 7.4 by using 10 mM HEPES buffer solution.

Kinetic behavior:

Fig S3(a) represents the changes of emission at different time interval by addition of F^- .

From the time vs. emission intensity plot (Fig.S3(a)) and linear detection range at fixed wavelength at 486 nm by using pseudo first order rate equation we get the rate constant $K = \text{slope} \times 2.303 = 0.00873 \times 2.303 = 2.01 \times 10^{-2} \text{ Sec}^{-1}$.

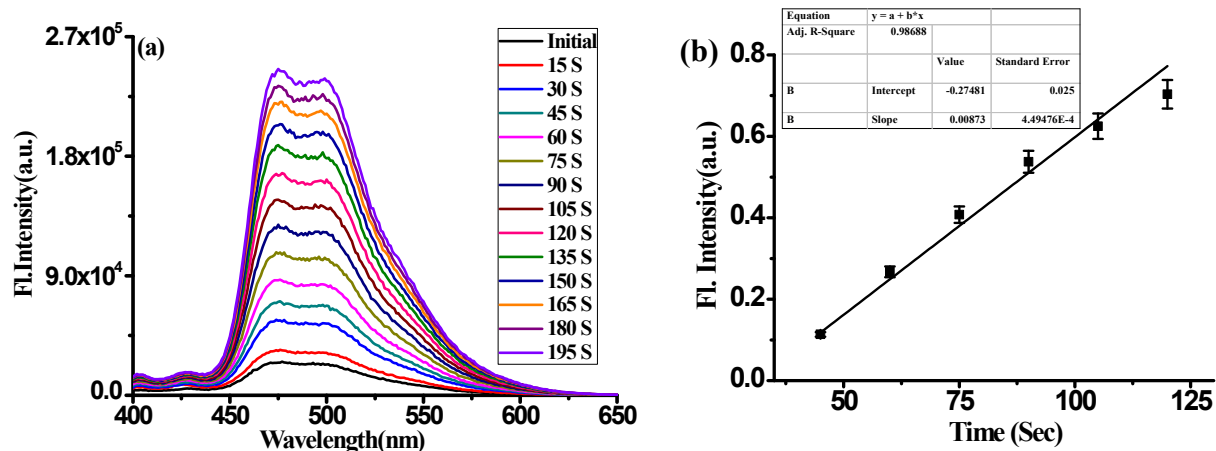


Figure S3: (a) The changes of emission spectra at different time intervals of **BSNA** in presence of F^- in CH_3CN : HEPES buffer solution (v:v, 5:5) at pH 7.4. **Inset:** Different time intervals are shown in the rectangle ('S' denotes Second). (b) The first order rate equation by using Time vs. fluorescent intensity plot at 486 nm.

Fig S4 (a) represents the changes of emission at different time interval by addition of DCNP to the **BBCI** solution.

From the time vs. emission intensity plot (Fig.S4 (b)) and linear detection range at fixed wavelength at 480 nm by using pseudo first order rate equation we get the rate constant $K = \text{slope} \times 2.303 = 0.00595 \times 2.303 = 1.4 \times 10^{-2} \text{ Sec}^{-1}$.

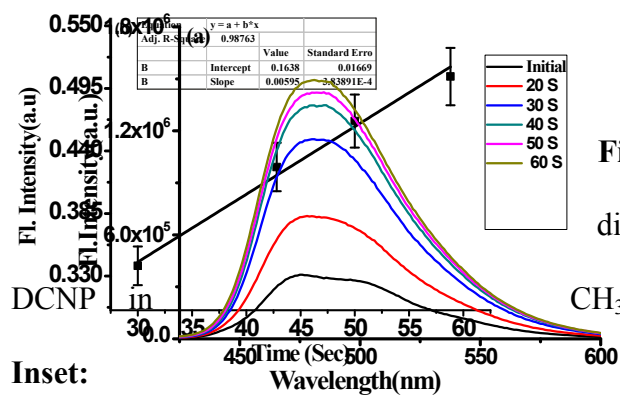


Figure S4: (a) The changes of emission spectra at different time intervals of **BBCI** in presence of **CH₃CN**: **HEPES** buffer solution (v:v, 5:5) at pH 7.4.

Inset:

Different time intervals are shown in the rectangle ('S' denotes Second). (b) The first order rate equation by using Time vs. fluorescent intensity plot at 480 nm.

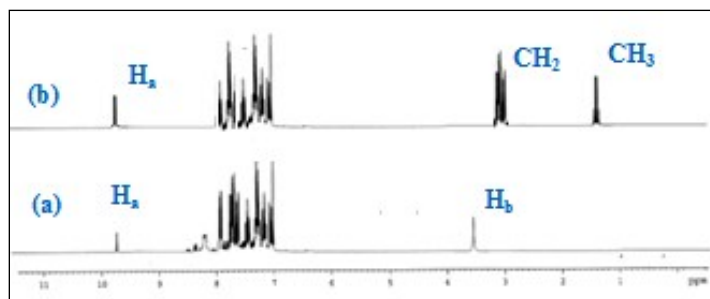
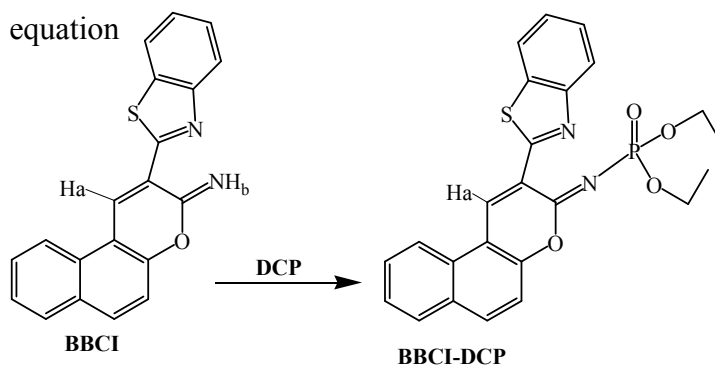


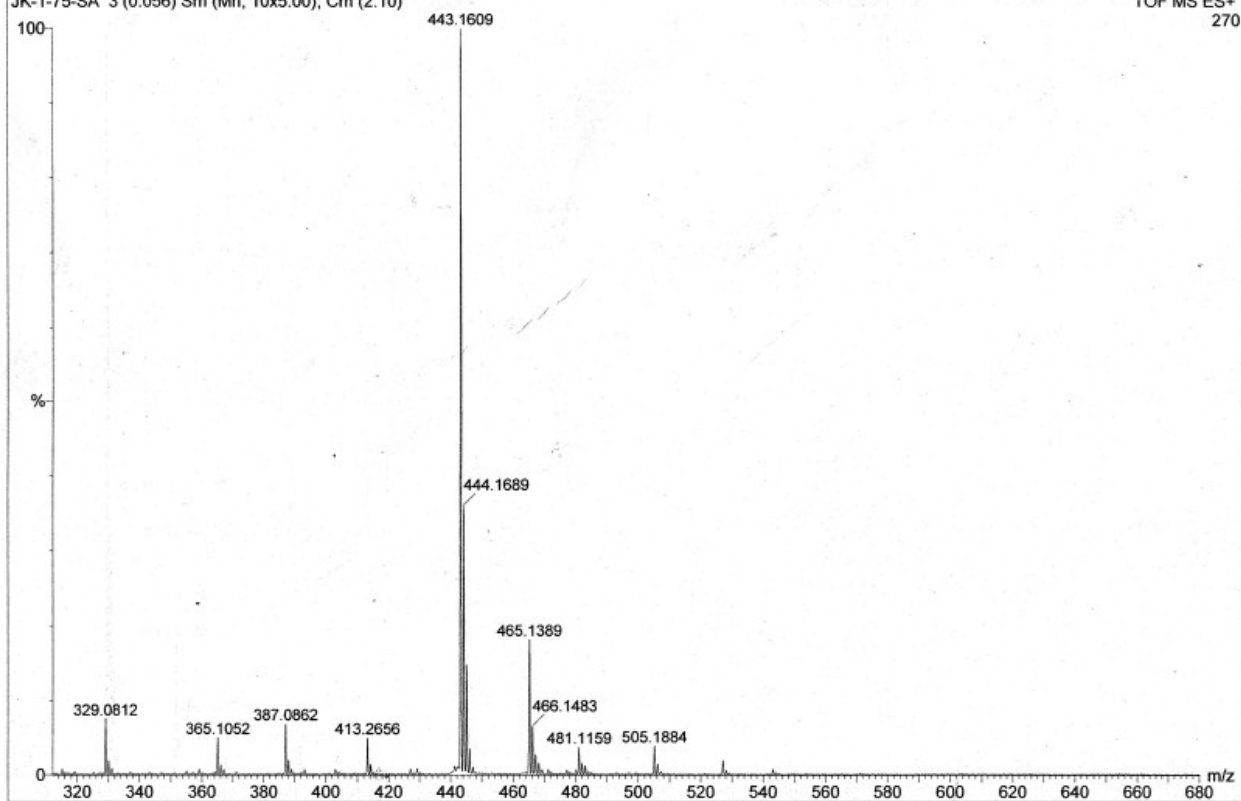
Figure S5: Comparison of partial ¹H-NMR spectra of (a) **BBCI**; (c) **BBCI+DCP** in **CDCl₃**.

¹H NMR spectra (S6) of BSNA:

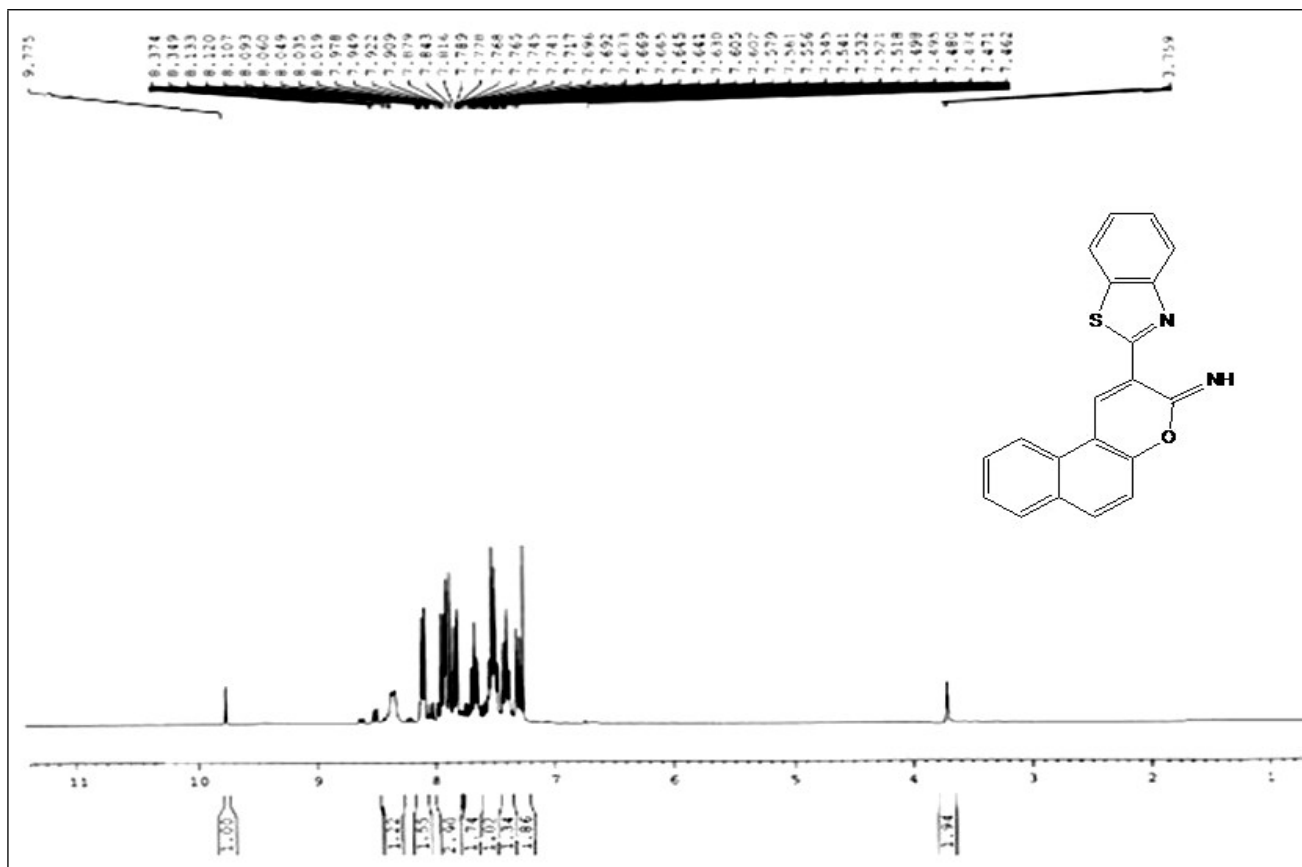
JK-1-75-SA-SKS

JK-1-75-SA 3 (0.056) Sm (Mn, 10x5.00); Cm (2:10)

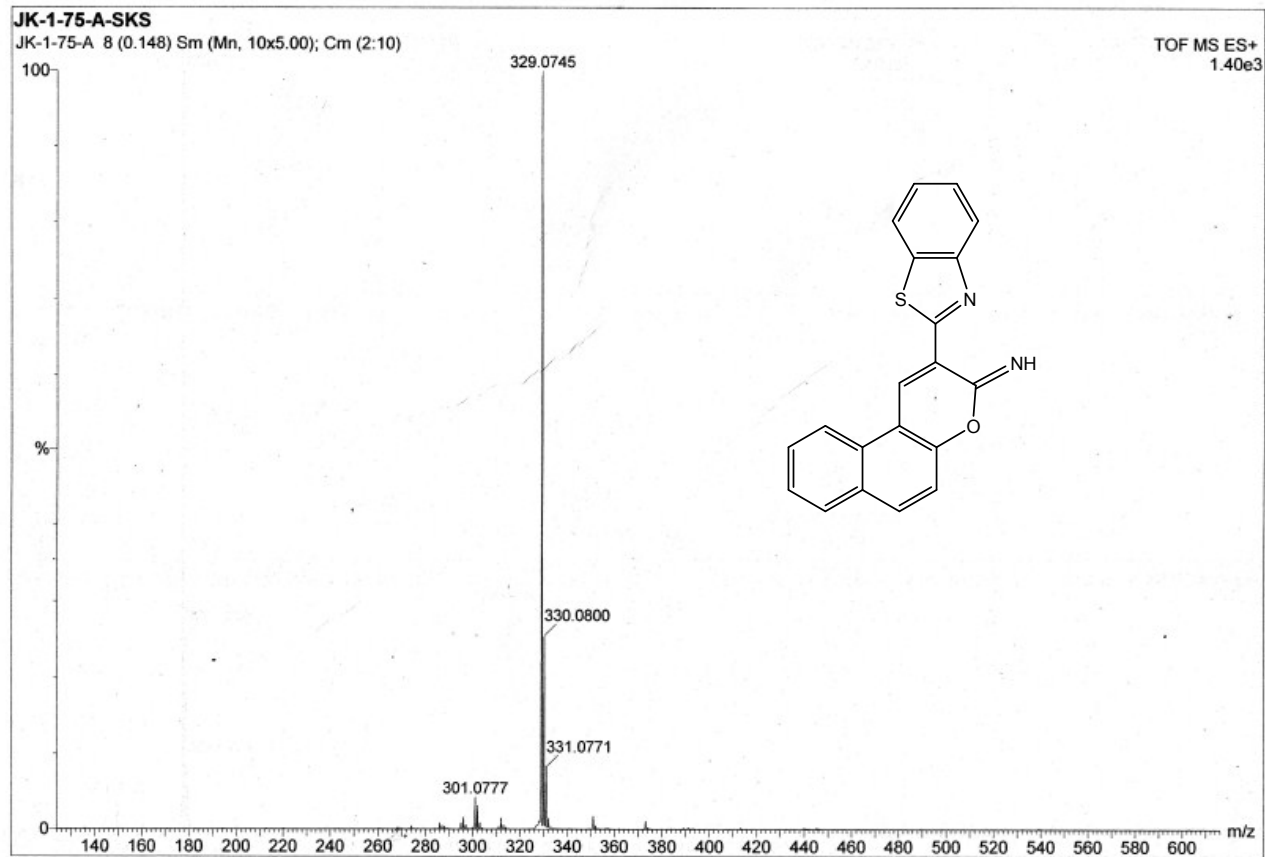
TOF MS ES+
270



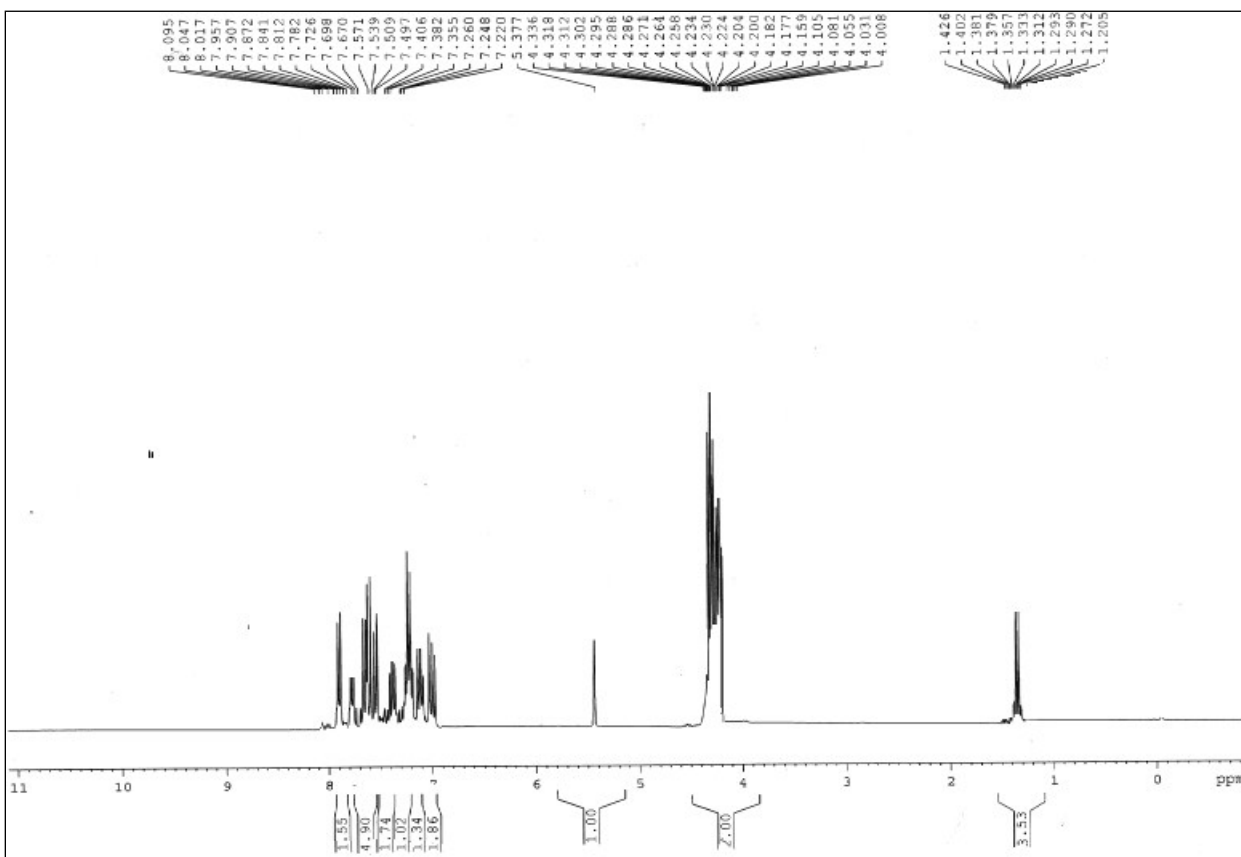
¹H NMR spectra (S8) of BBCI:



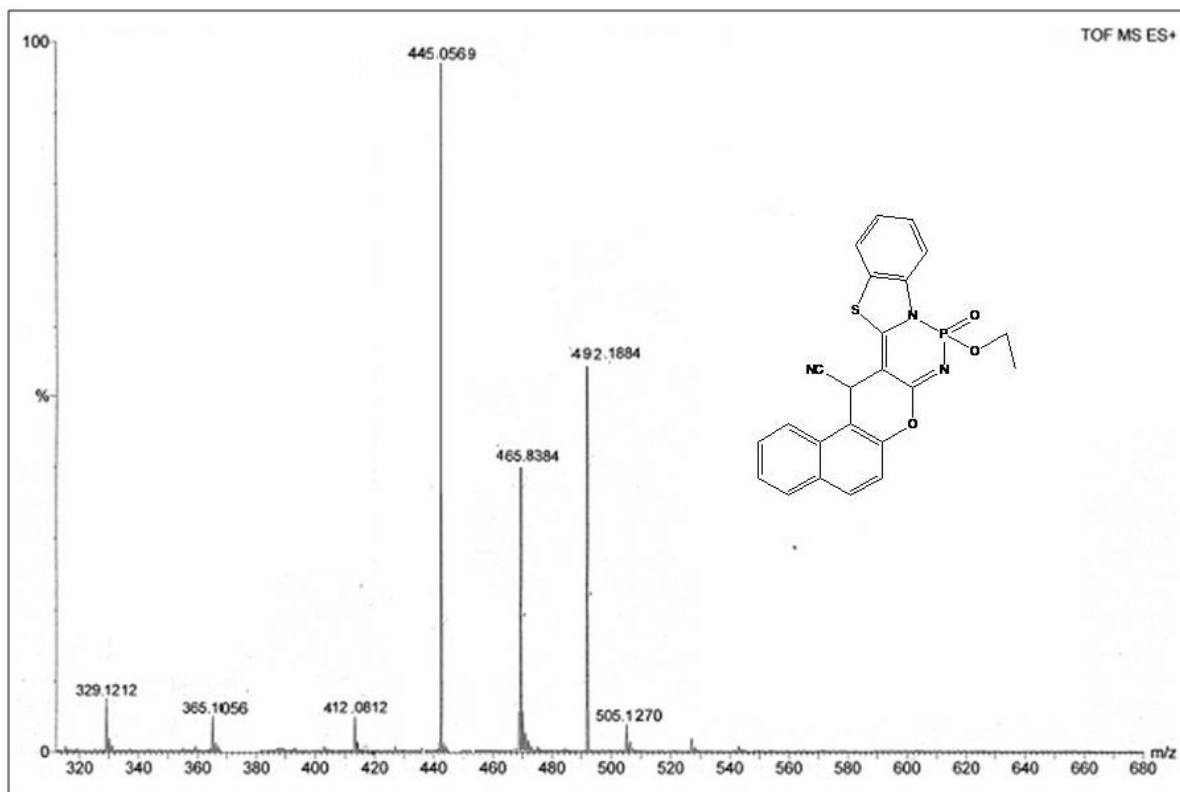
Mass spectra (S9) of BBCI:



¹H NMR spectra (S10) of BBCI+DCNP adduct:



Mass spectra (S11) of the resulting product BBCI+DCNP:



X-ray Crystallography:

Crystal structure of the **BBCI** was determined by single crystal X-ray diffraction from data collected at room temperature. A single crystal of $0.54 \times 0.14 \times 0.09 \text{ mm}^3$ in size was mounted on a glass fibre with epoxy cement for X-ray crystallographic study. The data were collected using a Bruker APEX II DUO CCD diffractometer with the graphite monochromated MoK α radiation at a detector distance of 5 cm and with APEX II software. The collected data were reduced using SAINT program and the empirical absorption corrections were performed using the SADABS program. The structure was solved by direct methods and refined by least-squares using the SHELXTL software package. All non-hydrogen atoms were refined anisotropically whereas hydrogen atoms were refined isotropically. The position of the N-bound H atom was located in a difference Fourier map and refined as a riding atom: N—H = 0.8602 Å with $U_{\text{iso}}(\text{H}) = 1.5 U_{\text{eq}}(\text{N})$. The C-bound H atoms were positioned geometrically and refined using a riding model: C—H = 0.93 Å with $U_{\text{iso}}(\text{H}) = 1.2 U_{\text{eq}}(\text{C})$. Two outlier reflections, 2 1 1 and 3 5 6, were omitted from the refinement. Crystallographic data for FS397 are presented in Table X1 and has been deposited with the Cambridge Crystallographic Data Center No. CCDC 1415425.

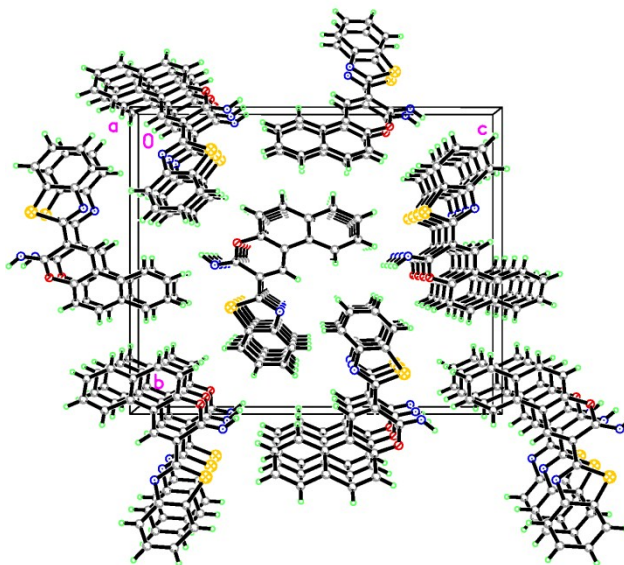


Figure S12: The crystal packing, viewed along the a axis, showing the molecules are stacked along the $[100]$.

Table S1: Experimental details

Crystal data (CCDC 1415425)	
Chemical formula	$C_{20}H_{12}N_2OS$
M_r	328.38
Crystal system, space group	Orthorhombic, $P2_12_12_1$
Temperature (K)	294
a, b, c (Å)	4.6985 (4), 16.2304 (13), 19.7042 (15)
V (Å ³)	1502.6 (2)
Z	4
Radiation type	Mo $K\alpha$
μ (mm ⁻¹)	0.22
Crystal size (mm)	$0.54 \times 0.14 \times 0.09$

Data collection	
Diffractionmeter	Bruker <i>SMART APEX II</i> DUO CCD area-detector diffractometer
Absorption correction	Multi-scan (<i>SADABS</i> ; Bruker, 2009)
T_{\min} , T_{\max}	0.886, 0.981
No. of measured, independent and observed [$I > 2\sigma(I)$] reflections	14735, 3684, 3232
R_{int}	0.033
$(\sin \theta/\lambda)_{\text{max}}$ (\AA^{-1})	0.665
Refinement	
$R[F^2 > 2\sigma(F^2)]$, $wR(F^2)$, S	0.034, 0.084, 1.03
No. of reflections	3684
No. of parameters	217
H-atom treatment	H-atom parameters constrained
$\Delta\rho_{\text{max}}$, $\Delta\rho_{\text{min}}$ (e \AA^{-3})	0.18, -0.14
Absolute structure	Flack x determined using 1226 quotients $[(I^+)-(I^-)]/[(I^+)+(I^-)]$ (Parsons, Flack and Wagner, <i>Acta Cryst. B</i> 69 (2013) 249-259).
Absolute structure parameter	-0.07 (3)

References:

- (a) Reddi, A. R.; Guzman, T. R.; Breece, R. M.; Tiemey, D. L.; Gibney, B. R.; *J. Am. Chem. Soc.*, **2007**, *129*, 12815–12827. (b) Lohani, C. R.; Kim, J-M.; Chung, S-Y.; Yoon, J.; Lee, K-H.; *Analyst*, **2010**, *135*, 2079-2084.